

# The role of size in the multiple scattering correction C for dual-spot aethalometer: a field and laboratory investigation – Supplementary Information

Laura Renzi<sup>1</sup>, Claudia Di Biagio<sup>2</sup>, Johannes Heuser<sup>3</sup>, Marco Zanatta<sup>1,2</sup>, Mathieu Cazaunau<sup>3</sup>, Antonin Bergé<sup>2</sup>, Edouard Panguì<sup>3</sup>, Jérôme Yon<sup>4</sup>, Tommaso Isolabella<sup>5,6</sup>, Dario Massabò<sup>5,6</sup>, Virginia Vernocchi<sup>6</sup>, Martina Mazzini<sup>1</sup>, Chenjie Yu<sup>2</sup>, Paola Formenti<sup>2</sup>, Benedicte Picquet-Varrault<sup>3</sup>, Jean-Francois Doussin<sup>3</sup>, Angela Marinoni<sup>1</sup>

<sup>1</sup> Institute of Atmospheric Sciences and Climate, National Research Council of Italy, Bologna, Italy

<sup>2</sup> Université Paris Cité and Univ Paris Est Creteil, CNRS, LISA, F-75013 Paris, France

<sup>3</sup> Univ Paris Est Creteil and Université Paris Cité, CNRS, LISA, F-94010 Créteil, France

<sup>4</sup> INSA Rouen Normandie, Univ. Rouen Normandie, CNRS, Normandie Univ., CORIA UMR 6614, 76000, Rouen France

<sup>5</sup> Department of Physics, University of Genoa, Via Dodecaneso 33, 16146 Genoa, Italy

<sup>6</sup> INFN – Division of Genoa, Via Dodecaneso 33, 16146 Genova, Italy

Correspondence to: Laura Renzi ([l.renzi@isac.cnr.it](mailto:l.renzi@isac.cnr.it))

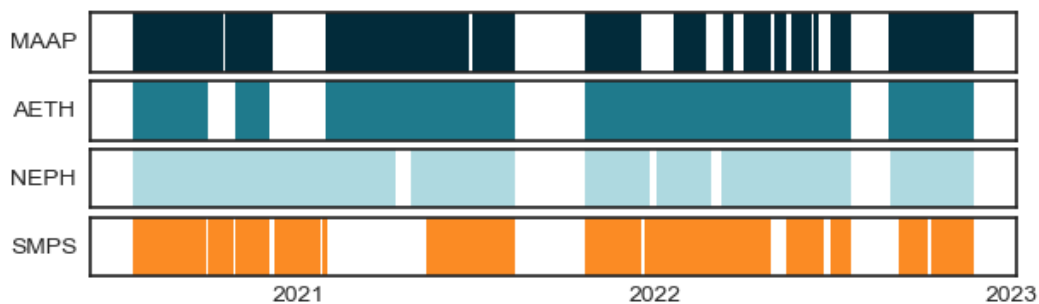


**Figure S1:** Instrument availability at CMN for MAAP, Nephelometer, Aethalometer and SMPS.

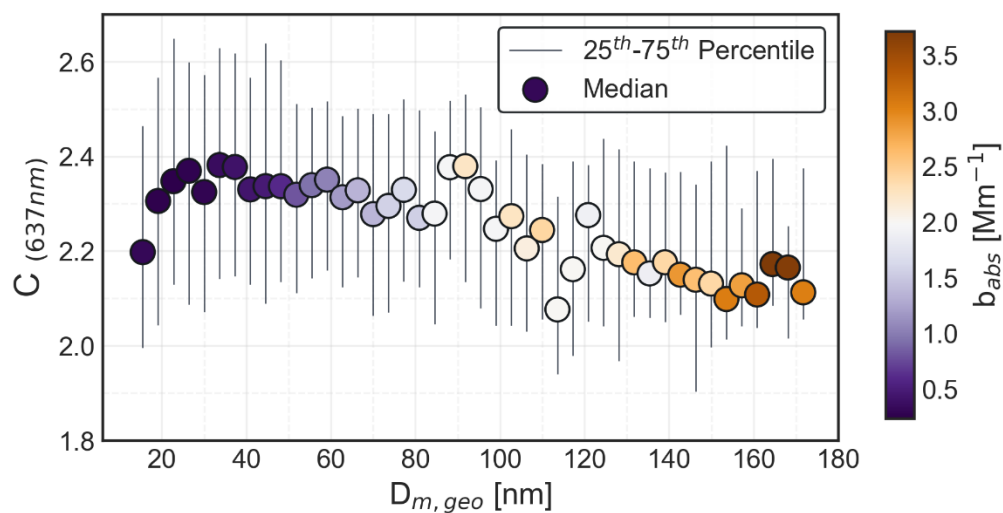


**Figure S2:** Cross-sensitivity of the C-size dependence on absorption coefficient measured by the MAAP. The color of the dots follows the variability of the median absorption coefficient in each size bin.

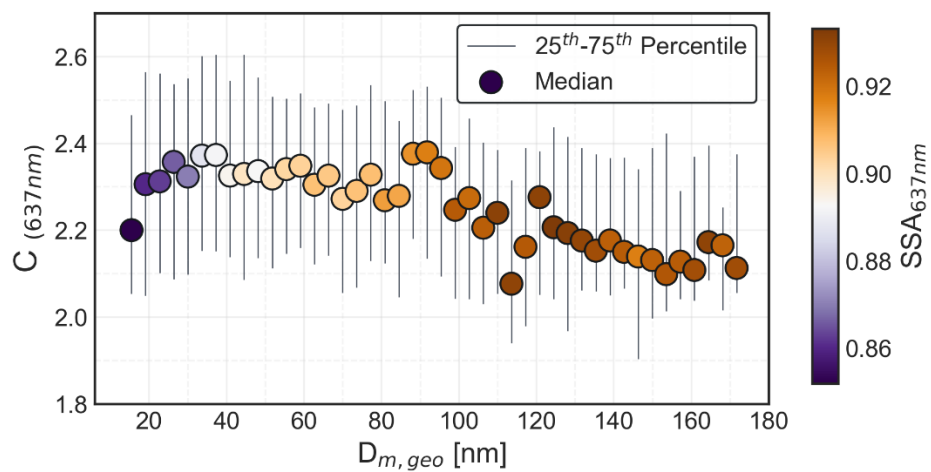


**Figure S3:** Cross-sensitivity of the C-size dependence on the SSA. The color of the dots follows the variability of the median SSA in each size bin.

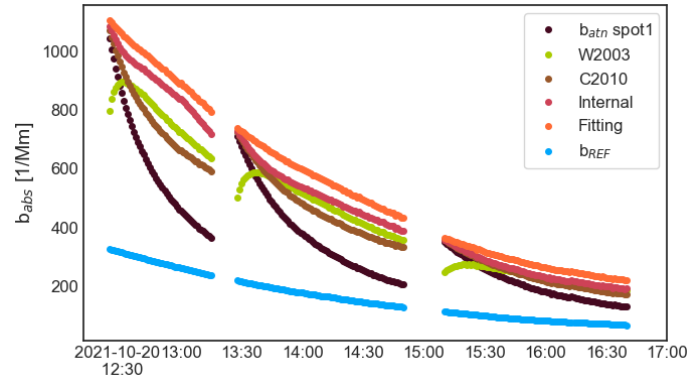


**Figure S4:** Variation of  $b_{atn}$  and  $b_{abs}$  at one-minute resolution during a representative chamber experiment. The periods of interruption in the series correspond to the aethalometer filter changes. The lightblue line represents the reference measurement, the dark brown line represents the attenuation coefficient uncorrected for loading, measured from spot 1 of the aethalometer at 660 nm, while the brown, green, red, and orange lines represent the loading-corrected attenuation coefficient using the C2010, W2003, Internal method, and Fitting methods, respectively.

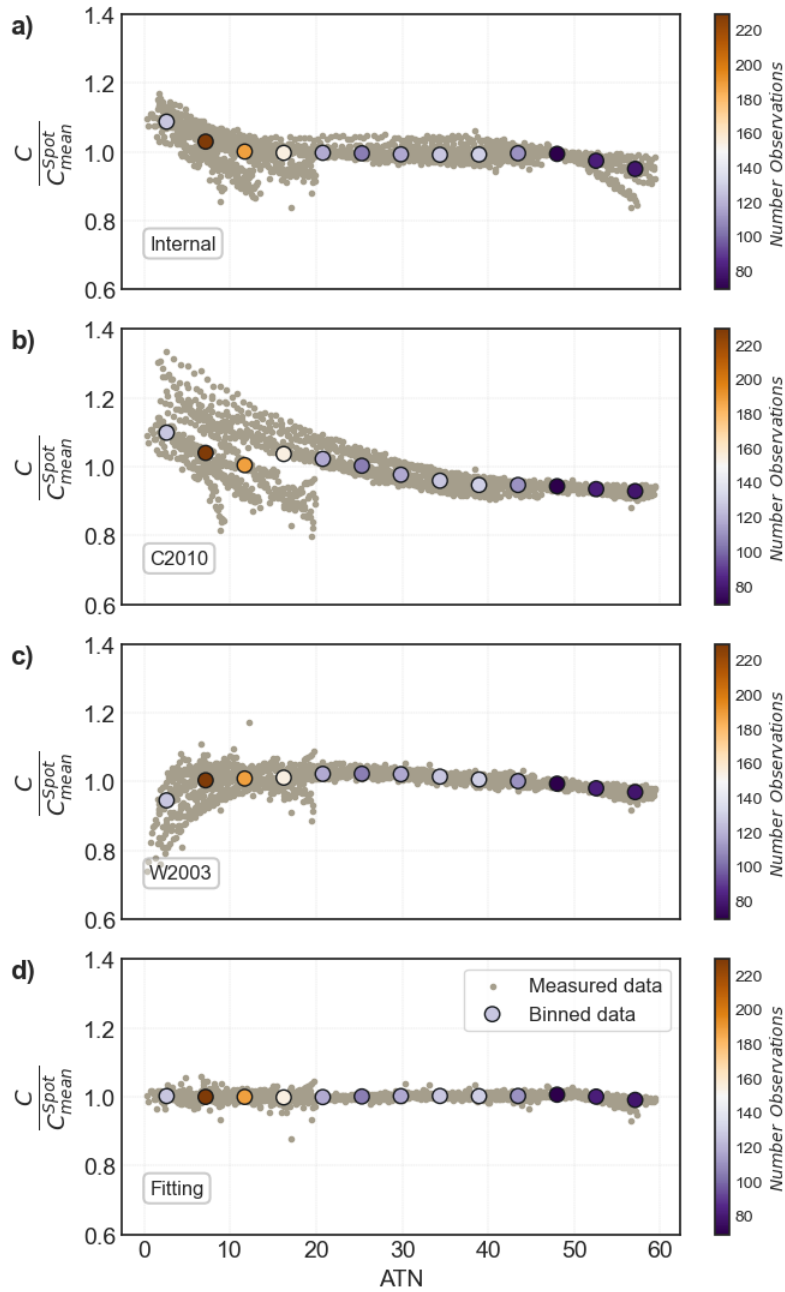


**Figure S5:** Variability of C values normalized for their average in each filter spot with attenuation at 660 nm. The grey points represent the one-minute resolution C values, while the colored points indicate the median values for each attenuation bin. The color intensity corresponds to the number of data points within each bin, providing a clear visualization of the data distribution. Data correspond to all CS1-CS5 experiments.

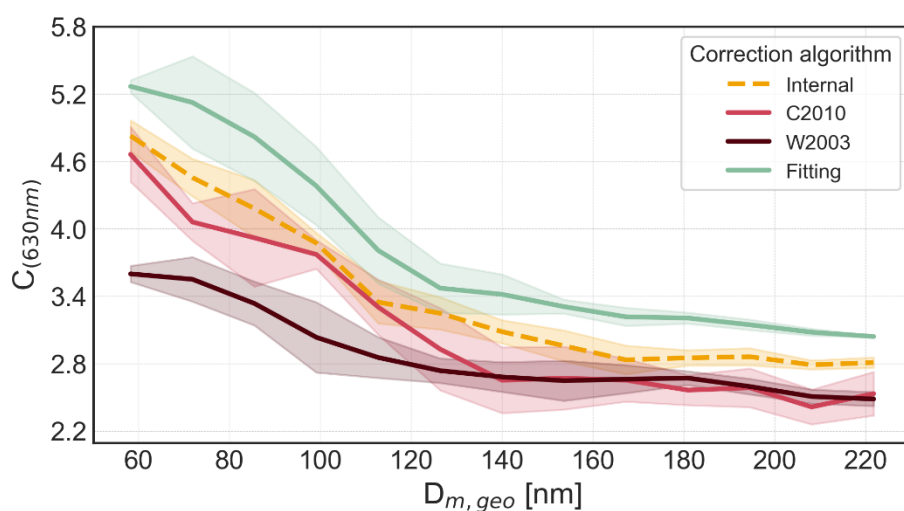


**Figure S6:** C dependence on particle size in laboratory studies. One-minute resolution C values are binned on the geometric mean diameter  $D_{m,geo}$ . The line represents the mean values in each bin the coloured area the mean  $\pm$  the standard deviation. One line is displayed for the C values derived from  $b_{atn,LC}$  loading corrected using different methods (Internal, C2010, W2003 and the 'Fitting' method).

58 **Table S1.** Physico-chemical properties of the Cast Soot (CS) aerosols for the five combustion conditions considered in  
59 this study (CS1 to CS5) corresponding to the first five predefined miniCAST operation points (OP1 to OP5) (Heuser et  
60 al., 2024).

Cast Soot Type	miniCAST flowrates fuel/mix. N <sub>2</sub> /ox. Air [L min <sup>-1</sup> ]	Combustion condition	Global equivalence ratio ( $\phi$ )	CMD <sub>60mi</sub> n ( $D_m$ ) [nm]	Mobility exponent ( $D_{fm}$ )	Fractal dimension ( $D_f$ )	Avg. Primary particle diameter ( $D_{pp}$ ) [nm]	EC/TC
CS1 (OP1)	0.03/0/0.75	Fuel lean	0.91	145 ± 12	2.11 ± 0.04	1.91 ± 0.22	9.8 ± 1.9	0.79 ± 0.11
CS2 (OP2)	0.025/0/0.60	Fuel lean	0.95	138 ± 1	2.10 ± 0.04	2.04 ± 0.24	7.2 ± 2.5	0.73 ± 0.08
CS3 (OP3)	0.025/0.01/0.60	Fuel lean	0.95	122 ± 9	2.10 ± 0.04	1.79 ± 0.20	15.4 ± 1.9	0.67 ± 0.09
CS4 (OP4)	0.023/0.02/0.60	Fuel lean	0.88	103 ± 17	2.20 ± 0.04	1.83 ± 0.22	10.0 ± 1.7	0.53 ± 0.13
CS5 (OP5)	0.023/0.02/0.45	Fuel rich	1.20	79 ± 2	2.25 ± 0.04	–	–	0.00 ± 0.22

**Table S2.** Summary of experimental conditions investigated during simulation chamber experiments at the CESAM chamber. The acronym CS stands for Cast Soot and CS1 to CS5 refers to particles generated under the five setting points of the miniCAST summarized in Table S1. The concentration of the CS at the peak of the injection as derived from SMPS and CPMA measurements (see Text S1). The date and time of start/end refer to the time periods within each experiment used for absorption measurements. The averages considered for C calculation correspond then to each aethalometer filter spot change inside these periods. The time since CS injection in CESAM to which the start of the experiment correspond is indicated.

Experiment	CS concentration at peak ( $\mu\text{g m}^{-3}$ )	Date time start	Date time end	Time from injection (hh:mm)
CS1	$61 \pm 6$	2021-10-19 12:31	2021-10-19 17:00	01:21-05:50
CS1	$157 \pm 19^*$	2022-12-12 11:35	2022-12-12 11:56	01:14-01:35
CS1	$166 \pm 20^*$	2022-12-14 10:25	2022-12-14 11:41	00:24-01:40
CS1	$167 \pm 21^*$	2022-12-15 11:50	2022-12-15 12:31	00:21-01:02
CS1	$171 \pm 21^*$	2022-12-16 11:57	2022-12-16 12:47	00:46-01:36
CS2	$95 \pm 8$	2021-10-20 12:24	2021-10-20 16:41	00:46-05:03
CS3	$89 \pm 8$	2021-10-26 11:49	2021-10-26 15:45	00:46-04:42
CS3	$151 \pm 20^*$	2022-12-06 09:40	2022-12-06 11:28	00:20-02:08
CS3	$219 \pm 29^*$	2022-12-07 11:35	2022-12-07 12:19	01:07-01:51
CS4	$44 \pm 4$	2021-10-22 12:05	2021-10-22 16:59	01:15-06:09
CS5	$46 \pm 4$	2021-05-28 11:54	2021-05-28 13:08	01:29-03:23
CS5	$65 \pm 7$	2021-10-21 12:25	2021-10-21 14:12	00:11-01:58
CS5	$127 \pm 23^*$	2022-12-08 11:37	2022-12-08 13:15	00:05-01:43
CS5	$121 \pm 22^*$	2022-12-09 10:13	2022-12-09 11:50	00:11-01:48

\* average masses calculated using the two CAPS signals and the MECs provided in Heuser et al., 2025 for the CSs



**Table S3:** Average C values, and their standard deviations, determined from one-minute resolution attenuation coefficient and absorption coefficient values, corrected for the loading effect using different methods; AE33 internal correction, W2003, C2010 and an experiment fitting specifically obtained for this study.

Method	Internal correction	W2003	C2010	Fitting
Mean (SD)	3.16 (0.50)	2.77 (0.3)	2.88 (0.56)	3.54 (0.6)

## Text S1 Loading correction schemes applied to chamber experiments

For chamber experiments the internal AE33 correction can provide uncertain results due to high soot concentration, frequent filter changes (tens of minutes-few hours), operating conditions highly variable between experiments, and experiment durations relatively short. As illustrated in Fig. S4 the time variability of the  $b_{atn,LC}$  does not follow the same decreasing trend over time as the reference measurement. However, it shows a steeper decline before and after the filter change, with a more rapid decrease in these points, making the trend appear more abrupt and also discontinuous around the filter transition. In this case the AE33 data were re-corrected for loading effect. To do this, the AE33 was treated like a single-spot aethalometer. The  $b_{atn}$  for the first spot (the one with higher flow rate) at one-minute resolution are considered. Three approaches are used to estimate three sets of  $b_{atn,LC}$ :

- the W2003 correction scheme: this approach assumes that the real absorption is measured at 10% of ATN and that the loading effect, represented by the loading correction  $R_{W2003}$ , results in a logarithmic dependence of  $b_{atn}$  vs ATN through a factor  $f(\lambda)$  as follows:

$$b_{atn,LC,W2003}(\lambda) = \frac{b_{atn}(\lambda)}{R_{W2003}(\lambda)} = \frac{b_{atn}(\lambda)}{\left[\left(\frac{1}{f(\lambda)} - 1\right) \cdot \frac{\ln ATN(\lambda) - \ln(10\%)}{\ln(50\%) - \ln(10\%)} + 1\right]} \quad (S1)$$

The  $f(\lambda)$  function can be expressed as a function of the particles SSA as  $f(\lambda) = a(1 - SSA) + 1$  with  $a$  equal to 0.87 (450 nm) and 0.85 (660 nm) in W2003.

- the C2010 correction scheme: this formulation assumes no loading effect at 0% ATN and a linear relationship between  $b_{atn}$  and ATN. The  $b_{atn,LC,C2010}(\lambda)$  according to C2010 is obtained as:

$$b_{atn,LC,C2010}(\lambda) = \frac{b_{atn}(\lambda)}{R_{C2010}(\lambda)} = \frac{b_{atn}(\lambda)}{\left(\frac{1}{f(\lambda)} - 1\right) \cdot \frac{ATN(\lambda)}{50\%} + 1} \quad (S2)$$

where  $R_{C2010}$  is the loading correction expressed as in W2003 with  $a = 0.74$ .

- the last approach used is developed specifically for this study, hereafter referred as ‘fitting’. As a matter of fact, both W2003 and C2010 correction approaches results in  $b_{atn,LC}$  whose temporal variation does not follow the evolution of the mass concentration in the chamber (Figure S4). This correction is based on few assumptions that we considered valid for the studied experiments. In particular, the temporal variability of the loading-corrected attenuation coefficient measured by the aethalometer must match that of the reference technique. Therefore,  $C$  is considered approximately constant within a filter spot. This assumption is an acceptable approximation in the experiments considered, where the properties of the particles change slowly during each experiment, as reported by Heuser et al. (2024). The attenuation value at which the loading effect is negligible is 0. The best function representing the dependence of  $b_{atn}/b_{ref}$  on ATN in these assumption was a second degree polynomial equation. The  $b_{atn,LC,fitting}(\lambda)$  according to this fitting method is thus obtained as:

$$b_{atn,LC,fitting}(\lambda) = \frac{b_{atn}(\lambda) \cdot c_1}{a_1 \cdot ATN(\lambda)^2 + b_1 \cdot ATN(\lambda) + c_1} \quad (S3)$$

where the parameters  $a_1$ ,  $b_1$ ,  $c_1$  were obtained by fitting the ratio  $b_{atn}/b_{ref}$  on ATN, and were derived separately for any filter spot. The primary advantage of applying this method is that it completely flattens the dependence of the loading-corrected attenuation coefficient on attenuation, whereas other methods retain this dependence (Figure S5).

111 Additionally, it improves the continuity of the measured values between the end of one filter spot and the beginning  
112 of the next, eliminating any jumps in the values (Figure S4).

## 114 **Text S2 Dependence of C on the attenuation and loading correction scheme from chamber experiments**

115 The loading effect correction scheme is critical especially under high concentrations of absorbing species and by  
116 consequence it can affect the retrieved C. Particularly, biases can arise immediately before and after filter changes, despite  
117 the internal loading correction applied (Cuesta-Mosquera et al., 2021). To investigate this aspect, the potential residual  
118 dependence of C on attenuation is analyzed taking advantage of the measurements in controlled chamber conditions.  
119 Indeed, as shown by Heuser et al. (2024), the properties of the CS1-CS5 (size, SSA, MAC) varied little during a filter  
120 spot cycle, therefore for each filter spot interval C should theoretically be independent of attenuation if the loading effect  
121 has been properly corrected. The analysis of this dependence was performed using C values at 630 nm, derived with a  
122 time resolution of one minute from  $b_{\text{atn,LC,Internal}}$  (630 nm) normalized to the mean C value for each spot. The results are  
123 illustrated in Fig. S5 reporting the normalized C as a function of the attenuation at 660 nm for all data acquired during  
124 chamber experiments with CS1-CS5. In addition to the minute-by-minute data, binned values as a function of attenuation  
125 were generated using the Python function 'np.histogram\_bin\_edges' and the 'fd' method. Figure S5.a reveals that even  
126 after the internal correction applied in real-time by the aethalometer, a dependency of the C factor on attenuation remains  
127 evident. Specifically, the correction tends to be overestimated by up to 20% following a filter change when attenuation  
128 values are below 10. Conversely, C is underestimated by up to 20% before the next filter change, particularly at attenuation  
129 values exceeding 50. This residual dependency introduces a notable bias in the average C values, especially in scenarios  
130 where the absorption Ångstrom exponent is high, and filter changes occur at ATN values (660 nm) close to 10.

131 We examined the dependence of C on attenuation using data corrected for the loading effect through the other methods  
132 described in Sect. 2.2.1: W2003, C2010, and the fitting method. Results for these different correction algorithms are also  
133 shown in Fig. S4. The C2010 method (Figure S5.b) introduces significant bias, with a spread of up to 45% for C  
134 particularly below ATN of 20. The W2003 method (Figure S5.c) reduces this bias to approximately 35%, but still leaves  
135 notable inaccuracies, particularly at low attenuation values (<10). On the other hand, the fitting method proposed  
136 effectively eliminates the dependency, providing the most accurate corrections (Figure S5.d). This method also ensures  
137 smoother continuity of absorption coefficient values between consecutive filter spots in longer experiments with multiple  
138 filter changes under consistent conditions (Figure S4). Based on these findings, we applied the fitting method to all data  
139 for subsequent analyses. This approach minimizes potential biases when comparing average C values across different  
140 experiments and filter spots. However, it is important to note that this method may not be suitable for conditions with  
141 greater variability in particle properties, where the assumption of a constant C value over time may not hold.

## 143 **Text S3 Cross-sensitivity of the C-size dependence on the loading correction scheme**

144 Analysis of the cross-sensitivity of the C-size dependence on the loading correction scheme applied suggests that the C  
145 increase for decreasing sizes is evident regardless of the correction method used (Figure S6). The largest increase (88%)  
146 occurs with the C2010 method, while the smallest (44%) is seen with the W2003 method. The internal correction method  
147 and the fitting one developed in this study yield similar increases of 71% and 77%, respectively. However, for the internal  
148 correction method, the C increase is observed to start at larger diameters, extending to CS1–CS4 particles. In consequence,

149 with the internal correction, differences of  $C$  between CS types at similar sizes become negligible, suggesting that size  
150 remains the dominant factor.  
151